Werk

Jahr: 1975
Kollektion: fid.geo
Signatur: 8 Z NAT 2148:41
Digitalisiert: Niedersächsische Staats- und Universitätsbibliothek Göttingen
Werk Id: PPN1015067948_0041
PURL: http://resolver.sub.uni-goettingen.de/purl?PPN1015067948_0041

LOG Id: LOG_0013
LOG Titel: A compressed air gun accelerator for shock magnetization and demagnetization experiments up to 20 kbar
LOG Typ: article

Übergeordnetes Werk

Werk Id: PPN1015067948
PURL: http://resolver.sub.uni-goettingen.de/purl?PPN1015067948
OPAC: http://opac.sub.uni-goettingen.de/DB=1/PPN?PPN=1015067948

Contact

Niedersächsische Staats- und Universitätsbibliothek Göttingen
Georg-August-Universität Göttingen
Platz der Göttinger Sieben 1
37073 Göttingen
Germany
Email: gdz@sub.uni-goettingen.de

J. Geophys. 41, 13–22, 1975

A Compressed Air Gun Accelerator for Shock Magnetization and Demagnetization Experiments up to 20 kbar

U. Hornemann, J. Pohl, and U. Bleil

Institut für Angewandte Geophysik der Universität München

Received March 4, 1974

Abstract. For the investigation of the effect of stress waves on magnetic properties of rocks a non-magnetic compressed air gun accelerator was built. The stress waves are generated by planar impact of accelerated aluminium projectile plates on the rock samples. The velocity of the projectiles can be varied between about 15 m/s and 200 m/s. The stress amplitudes range from 1.5 to 20 kbar. The duration of the stress waves is of the order of several μs and can be varied by using projectiles of different thickness. The cylindrical rock samples have a maximum diameter of 2.5 cm and a length up to several cm. For basalt samples the stress is determined by using Hugoniot-data of basalt and aluminium and the impact velocity of the projectile. The stress wave profile is measured with piezo-ceramic transducers. The magnetic field at the place of the sample is controlled with a triple set of Helmholtz coils.

Key words: Rock Magnetism — Shock Magnetization — Shock Demagnetization — Piezomagnetic Effect — High Pressures.

1. Introduction

In an ambient magnetic field stress waves can produce a remanent magnetization in ferromagnetic materials (SRM, shock remanent magnetization), in zero field they can demagnetize ferromagnetic materials having a remanent magnetization (shock demagnetization).

For rocks containing ferromagnetic minerals these effects have been studied by several authors (Domen, 1961; Pohl, 1967; Hargraves and Perkins, 1969; Nagata, 1971). For the generation of the stress waves automatic hammering devices, falling masses or explosives were used. Generally the stresses did not exceed several hundred bar, exept when explosives were employed. In this case the stresses probably were of the order of tens of kilobars, but only qualitative informations could be obtained from the experiments.

It therefore seemed interesting to make quantitative measurements of the magnetizing and demagnetizing effect of stress waves in the higher stress range. For this purpose a non-magnetic compressed air gun accele-

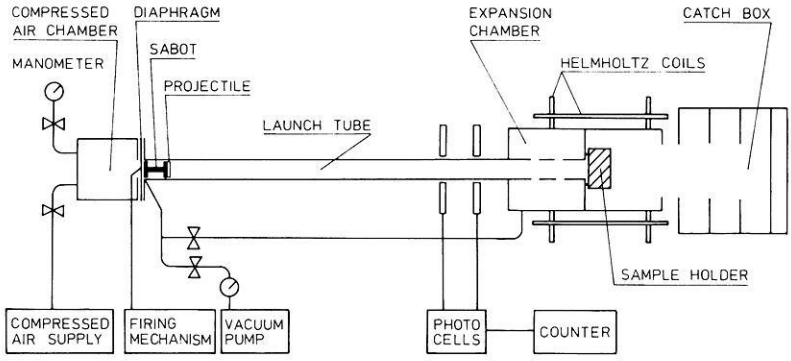

Fig. 1. Schematic view of the non-magnetic compressed air gun accelerator

rator was developed to generate stress waves of a duration of several μs with a maximum amplitude up to 20 kbar. In the following a description of the apparatus and the calibration for experiments with basaltic rocks will be given.

2. *The Compressed Air Gun Accelerator*

The apparatus consists mainly of a compressed air chamber and an evacuated launch tube separated by a diaphragm consisting of one or several thin plastic foils (Fig. 1). The launch tube has a length of 190 cm and an inner diameter of 3 cm. It is closed by the sample holder device, which adheres to the end of the evacuated tube by the atmospheric pressure. Over several slits at the end of the tube an expansion chamber is mounted to prevent compression of air in front of the accelerated projectile. At present 3 mm thick, flat grinded aluminium plates are used as projectiles. For acceleration they are pasted on a plastic sabot (Trovidur), which is designed to give an exact guidance to the projectile within the launch tube, thus providing a planar impact. The velocity of the projectile is measured with two photocells. It depends on the sabot and projectile mass and the pressure in the compressed air chamber. With a pressure of 5 bar a 50 g projectile is accelerated to a velocity of about 100 m/s at the end of the launch tube. The amplitude of the stress wave in the sample generated by the impact is determined by accelerating the projectile to an appropriate velocity. The desired velocity can be obtained with an accuracy better than 1%.

For an experiment the sabot with the projectile is placed just behind the diaphragm, the lauching tube and the expansion chamber are evacuated to a pressure less than 0.1 mbar; the compressed air chamber is filled, the diaphragm perforated with a match point and the sabot with the projectile

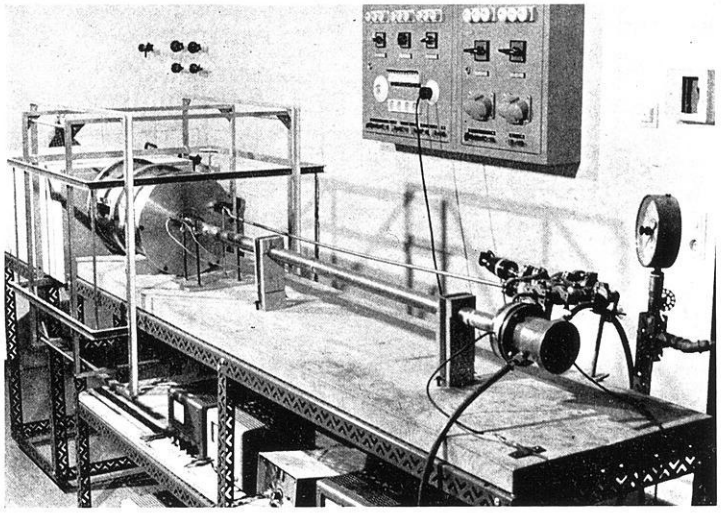

Fig. 2. The compressed air gun accelerator. To the right the compressed air chamber is shown, to the left the expansion chamber and a triple set of Helmholtz coils for the control of the magnetic environment

accelerates in the launch tube. The impact of the projectile on the sample holder device generates a stress wave in the sample. A catch box for the sample holder device filled with soft plastic material permits to avoid further shocks on the impacted sample.

In order to allow measurements of magnetic properties of the rocks, the launch tube, the expansion chamber and the sample holder device are made of non-magnetic materials (brass and aluminium). The sample holder is placed at the center of a triple set of Helmholtz coils which control the magnetic field at the place of the sample. The magnetic field in the laboratory can be compensated to ± 0.005 Oe and magnetic fields up to 10 Oe produced in various directions.

3. The Sample Holder Device

To prevent rapid crushing and demolition by the impact the basalt samples are mounted in a special sample holder device, which also provides a simple vacuum tightening of the launch tube (Fig. 3). The basalt samples have a cylindrical form 25 mm in diameter and 25 mm in length. They are pasted into a thin aluminium ring with an epoxy resin. The aluminium ring is fitted into a larger aluminium cylinder, which is closed on both sides with aluminium cover plates. After the impact the aluminium ring with the basalt sample can easily be removed from the aluminium cylinder for measure-

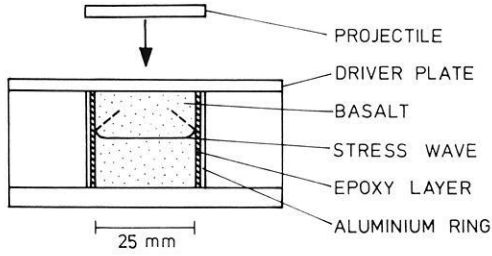

Fig. 3. Sample and sample holder device

ments of the magnetization and other magnetic experiments. The faces of the projectile, the cover plate and the basalt sample are face grinded to provide a good contact between the impacting projectile, the cover plate and the sample, which is necessary to assure a most ideal transmission of the stress wave.

4. *Determination of the Amplitude of the Stress Waves*

Stress waves generated by planar impact can be described in terms of the Rankine-Hugoniot equations for shock waves. These are obtained from the conservation laws for mass, momentum and energy across a single steady shock front in the one-dimensional case (Duvall and Fowles, 1963; for a discussion of the anisotropic stress distribution in stress waves see McQueen, *et al.* (1970)). The relation between stress σ and particle velocity u behind the stress wave front is given by:

$$\sigma = \varrho_0 \, u \, U \tag{1}$$

U — propagation velocity of the stress wave; ϱ_0 — initial density.

Experimental Hugoniot-Curves giving the relation between σ and u are known for aluminium and basalt (Fowles, 1961; Ahrens and Gregson, 1964; Ahrens, Petersen and Rosenberg, 1969). With these curves and the impact velocity v of the projectile on the driver plate it is possible to determine the stress σ in the basalt.

After the impact a stress wave runs from the interface projectile/driver plate into the driver plate and in opposite direction into the projectile. The momentum is partitionned and the particle velocity in the driver plate will be (Duvall and Fowles, 1963):

$$u = 1/2 \, v \, . \tag{2}$$

Knowing u we can determine the stress amplitude of the wave in the driver plate from the experimental Hugoniot-curve for aluminium (Fig. 4, $u_1 \rightarrow \sigma_1$).

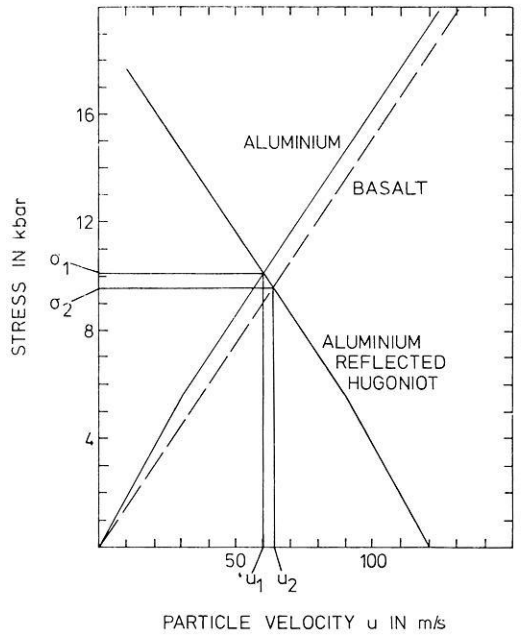

Fig. 4. Experimental Hugoniot-data for aluminium and basalt for the determination of the stress wave amplitude in basalt

At the interface driver plate/basalt the incident wave is partly transmitted and partly reflected as the basalt has a different impedance for stress waves. The relation between stress and particle velocity for the reflected wave in aluminum is given by the reflected Hugoniot-curve in Fig. 4. The amplitude σ_2 of the stress wave in the basalt is determined by the following boundary conditions: At the interface the resulting stress must be the same on both sides of the interface and the state of the interface must lie on both the reflected Hugoniot-curve for the driver plate through the point (u_1, σ_1) and on the Hugoniot curve for basalt. This yields the stress σ_2 and the particle velocity u_2 in the basalt. The graphical method to determine σ_2 is illustrated in Fig. 4. Due to the different wave impedances of aluminium and basalt the stress in the rock sample is about 0.5 kbar lower than in the aluminium driver plate.

By propagating through the basalt the amplitude of the stress wave decreases by about 20% on the distance of 25 mm (see section 5). Here only a short discussion of different mechanisms contributing to the amplitude decrease will be given. Absorption may be neglected on the short distance of 25 mm. The epoxy-resin layer acts as a side barrier for the wave energy. Divergence and thus an amplitude reduction of the initial plane stress wave

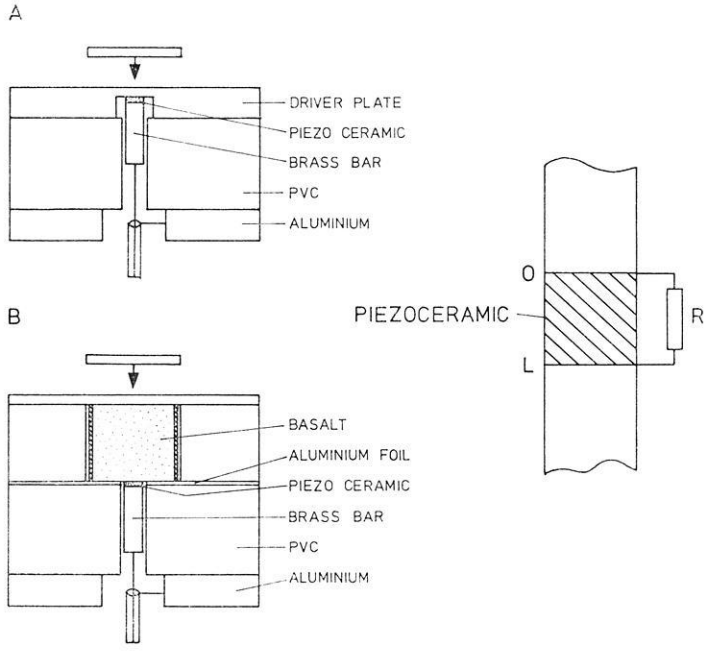

Fig. 5. Experimental devices for the measurement of stress wave forms with piezo-ceramic transducers (a) on the impact side and (b) on the back side of the basalt sample. Schematic diagram of the piezo-ceramic transducer

with increasing distance from the impacted surface is therefore highly suppressed. Only about 10% of the energy are thought to leave the sample. This causes a curvature of the wave front (Fig. 3). An additional effect may come from a weak oblique rarefaction wave reflected from the sides of the sample. A further reduction of the amplitude results from the faster moving back side rarefaction wave which overtakes the primary stress wave at a certain distance.

5. Measurement of the Wave Profile

The calculations in section 4 give only an information about the maximum amplitude of the stress wave but not on the wave profile. Therefore measurements of the stress wave form generated with the above described gun accelerator were made in the low stress range using piezoelectric ceramics with remanent polarization.

The piezoelectric element acts as a capacitor C which is charged by the stress wave travelling through. It is discharged through a resistance R connected in parallel (Fig. 5, one-dimensional case). The corresponding

voltage drop is measured with an oscilloscope. The piezoelectric polarization P is given by:

$$P = \sigma d \tag{3}$$

d — piezoelectric constant, $\sigma = \sigma(t)$ — stress.

The dielectric displacement D is

$$D = \varepsilon \varepsilon_0 E + \sigma d \tag{4}$$

ε, ε_0 — relative and absolute dielectric constant, E — electric field.

Integration over the length l of the piezo-element yields the following linear differential equation for the relation between the electric voltage $u(t)$ and the stress $\sigma(t)$ (Reibold, 1972):

$$C_0 \frac{du(t)}{dt} + \frac{u(t)}{R} - \frac{Fd}{\alpha}(\sigma(0, t) - \sigma(l, t)) = 0 \tag{5}$$

With the initial condition $u(0) = 0$ a general solution is

$$u(t) = \frac{Fd}{\alpha C_0} \int_0^t (\sigma(0, t') - \sigma(l, t'))\, e^{-\frac{T+\alpha-t'}{\tau}}\, dt' \tag{6}$$

T — signal length, α — travel time of the stress wave through the piezo-element, $\tau = R C_0$ — time constant of the measuring circuit, F — area of the piezo-element.

According to Reibold (1972) simple solutions of (6) can be obtained in special cases. For $\tau \gg T \gg \alpha$ the solution is

$$u(t) = \frac{F \cdot d}{C_0} \sigma(0, t) \tag{7}$$

This solution was used in the present case. The conditions $\tau \gg T \gg \alpha$ are satisfied with the short duration of the generated stress waves and by using thin ceramic plates. The impulse length T is of the order of 10 to 25 μs with the maximum amplitude lasting no longer than about 1 μs. The piezo-ceramic elements have a diameter of 5.7 mm and a thickness of 0.4 mm. With a sound velocity of 4.3 km/s the travel time through the plate is estimated to 0.1 μs. The total capacity C_0 of the measuring circuit system (capacities of the piezo-ceramic element, connecting cable and input of the oscilloscope) is 700 pF. With a resistance R of 1 MΩ the time constant τ is about 60 s. The piezo-ceramic material is a lead zirconate-titanate Sonox I (Stemag AG, Lauf, W.-Germany) with the following characteristics:

Density	ϱ	7.6	g/cm³
Young's modulus	E	$10.7 \cdot 10^{-10}$	N/m^2
Piezo-electric charge constant	d_{33}	$150 \cdot 10^{-12}$	C/N
Relative dielectric constant	ε	650	—
Frequency constant (thickness expansion)	N_T	2.15	kHz · m
Curie temperature	T_C	410	°C

Non-linearities are neglected.

Fig. 5 shows the two measuring arrangements for the wave profile at the front side and the back side of the sample. The piezo-ceramic discs are mounted with an electroconductive epoxy resin. In order to avoid reflections at the back side of the ceramic plate a brass bar 25 mm long is pasted on the ceramic plate with the same epoxy resin. The thickness of the epoxy film does not exceed 0.02 mm. The length of the brass bar provides about 12 μs measuring time without disturbance by a reflected wave from its free end. The capacitor electrodes of the ceramic plate are connected with coaxial cables to an oscilloscope.

Measured stress wave profiles are shown in Figs. 6a and 6b .The impact velocities are $v = 18.8$ m/s for Fig. 6a and $v = 18.2$ m/s for Fig. 6b. The stress impulse measured just behind the driver plate is thought to be similar to the impulse in the basalt near the impacted surface. In front of the basalt sample the duration T of the stress impulse is about 8 μs and the rise time about 1 μs. The secondary peak about 2 μs after the first maximum is, as travel time calculations show, due to the reflected wave from the back side of the 3 mm thick projectile. The integral $\int \sigma \, dt$ over the impulse gives the momentum per unit surface. It is in good agreement with the theoretical half momentum per unit surface of the impacting projectile.

On the back side of the basalt sample the impulse length is about 25 μs with a rise time of 10 μs. The broadening of the impulse is to a great deal due to waves reflected from the boundaries of the experimental arrangement. Thus for example the small peak observed in the broad maximum is caused by a wave reflected at the end of the brass bar. The delay time of about 12 μs corresponds to the travel time through the brass bar.

From the measured voltage the amplitude σ_{exp} of the stress wave may be estimated with relation (7). For Figs. 6a and 6b we have $\sigma_{\text{exp}} = 1.50$ kbar and $\sigma_{\text{exp}} = 1.19$ kbar respectively. The amplitudes σ_{theor} deduced from the impact velocities as described in section 4 give for the same experimental arrangements $\sigma_{\text{theor}} = 1.74$ kbar and $\sigma_{\text{theor}} = 1.50$ kbar. The stress obtained with the piezo-ceramic transducers is about 15 to 20% lower than the values deduced from the impact velocities. Several factors may account for this difference. For the calculation of the stress amplitudes in the

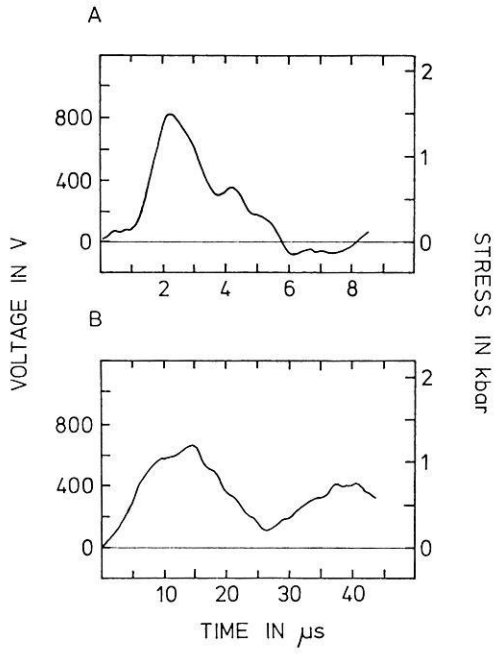

Fig. 6. Stress wave form (A) on the impact and (B) on the back side of a basalt sample

basalt a purely one-dimensional wave propagation was assumed. Especially for the back side of the basalt sample this method can only give approximate results. The boundary conditions for the interfaces aluminium/piezo-ceramic and basalt/piezo-ceramic are not considered as Hugoniot-curves for the ceramics used are not known. Furthermore it is assumed that the piezoelectric polarization is proportional to the stress although this relation is not linear in the high stress range. Finally the reciprocal piezoelectrical effect in lead zirconate-titanate also contributes to reduce the measured voltage. As a result we estimate that the stress values calculated from the impact velocities should be reduced by about 5 to 10%.

Acknowledgements. We wish to thank Prof. G. Angenheister, director of the Institut für Angewandte Geophysik, University of Munich, for his encouragement and support. We are also grateful to Dr. N. Petersen, Dr. A. Schult and Prof. H. Soffel for valuable discussions. Special thanks are due to A. Krumm and B. Nasdala, Weil, for preparation of the sample holder devices and for assistance in making the impact experiments. The financial support of the Deutsche Forschungsgemeinschaft is gratefully acknowledged.

References

Ahrens, T. J., Gregson, V. G.: Shock compression of crustal rocks: Data for quartz, calcite, and plagioclase rocks. J. Geophys. Res. *69*, 4839–4873, 1964

Ahrens, T. J., Petersen, C. F., Rosenberg, J. T.: Shock compression of feldspars. J. Geophys. Res. *74*, 2727–2746, 1969

Domen, H.: A note on remanent magnetism caused by impulsive pressure. Bull. Fac. Educ. Yamaguchi Univ. *10*, 71–76, 1961

Duvall, G. E., Fowles, G. R.: Shock waves. High pressure physics and chemistry. R. S. Bradley, ed. London: Academic Press 1963

Fowles, G. R.: Shock wave compression of hardened and annealed 2024 aluminium. J. Appl. Phys. *32*, 1475–1487, 1961

Hargraves, R. B., Perkins, W. E.: Investigations of the effect of shock on natural remanent magnetism. J. Geophys. Res. *74*, 2576–2589, 1969

McQueen, R. G., Marsh, S. P., Taylor, J. W., Fritz, J. N., Carter, W. J.: The equation of state of solids from shock wave studies. High-velocity impact phenomena, R. Kinslow, ed. New York: Academic Press 1970

Nagata, T.: Introductory notes on shock remanent magnetization and shock demagnetization of igneous rocks. Pageoph *89*, 159–177, 1971

Pohl, J.: Magnetisierung und Entmagnetisierung von Stahl und Magnetit durch Stoßwellen. Unpublished report, Institut für Angewandte Geophysik, University of Munich, 1967

Reibold, R.: Piezoelektrische Wandler zur Untersuchung mechanischer Kurzzeitbelastungen. Acustica *27*, 189–196, 1972

Dr. U. Hornemann
Arbeitsgruppe für
Ballistische Forschung
D-7858 Weil
Hauptstr. 18
Federal Republic of Germany

Dr. J. Pohl
Institut für Angewandte Geophysik
der Universität
D-8000 München 2
Theresienstr. 41
Federal Republic of Germany

Dr. U. Bleil
Institut für Geophysik
der Ruhr-Universität
D-4630 Bochum
Buscheystrasse
Federal Republic of Germany